Universality and scaling in two-step epitaxial growth in one dimension

V. I. Tokar and H. Dreyssé
IPCMS, Université de Strasbourg-CNRS, UMR 7504, 23 rue du Loess, F-67034 Strasbourg, France
(Received 5 September 2015; published 28 December 2015)

Irreversible one-dimensional (1D) epitaxial growth at small coverages via the recently suggested two-step growth protocol [Tokar and Dreyssé, Surf. Sci. **637-638**, 116 (2015)] has been studied with the use of the kinetic Monte Carlo and the rate-equation techniques. It has been found that similar to the two-dimensional (2D) case the island capture zones could be accurately approximated with the Gamma probability distribution (GD). Coverage independence of the average island sizes grown at the first step that was also found in two dimensions was observed. In contrast to 2D case, the shape parameter of the GD was also found to be coverage-independent. Using these two constants as the input, an analytical approach that allowed for the description of the commonly studied statistical distributions to the accuracy of about 2% has been developed. Furthermore, it was established that the distributions of the island sizes and the interisland gaps grown via the two-step protocol were about 50% narrower than in the case of nucleation on random defects, which can be of practical importance. Equivalence between the GD shape of the island size distribution in the scaling regime and the linear dependence of the capture numbers on the island size in the rate-equation approach has been proved.

DOI: 10.1103/PhysRevE.92.062407 PACS number(s): 81.15.Aa, 68.55.A−

I. INTRODUCTION

Scaling behavior of various size distributions measured in the kinetic Monte Carlo (KMC) studies of the irreversible epitaxial growth has been the subject of extensive study over the past three decades [1–8]. It has been established that under the standard growth setup (SGS) when the atoms are deposited on an initially clean surface in a single run at a constant deposition rate, the scaling observed was only approximate [1–3,5–9]. This does not undermine its significance because, as we know from the renormalization group theory, the deviations from scaling may provide such vital information as the critical indexes [10]. Thus, it may be hoped that the approximate character of the scaling in the epitaxial growth means that the simulated systems are close to criticality, but some relevant variables still deviate from their critical values. Identification of the variables and accounting for the deviations from scaling could lead to the development of the growth theory similar to the renormalization group description of the critical phenomena.

Despite continuing efforts, however, a theory of this kind has not yet been developed. A major obstacle to theoretical description of the growth under the SGS poses the necessity to account for the island nucleation that takes place during the whole deposition run (see Refs. [3,5] and references therein). The intertwining of the nucleation and the aggregation phenomena makes the growth process extremely intricate, so that even in the one-dimensional (1D) case its theoretical description poses highly nontrivial problems [5].

As will be shown below, the two-step growth setup (2SGS) [11] where the island nucleation is restricted mainly to the first growth step with the second step being dominated by the aggregation, the aggregation behavior became much simpler. This is because in the absence of nucleation the capture zone distribution (CZD) [3] remains unchanged at least in the case of the point islands. So when the average island size becomes sufficiently large and the finite-size statistical fluctuations become negligible, the island size distribution (ISD) scales as the CZD [12]. This simplifies the identification of relevant variables that hamper the scaling behavior at the second growth step.

The aim of this paper is to study the irreversible growth in the 2SGS in the precoalescence regime in 1D models and to show that the growth can be accurately described with the use of only two constants: the average size of the islands nucleated at the first growth step and the shape parameter of the Gamma distribution (GD) that characterizes the CZD and the gap size distribution. This is the main empirical finding of our study. Previously [11], we established similar result for the 2SGS in two dimensions. But, first, the topology of 1D and two-dimensional (2D) spaces is very different, so the two findings though similar are independent. Second, the shape parameters of the GDs in two dimensions were coverage-dependent, while in one dimension the shape parameter has universal value for all sufficiently small values of the coverage. The existence of simple analytic expressions for size distributions is very convenient from both theoretical and experimental points of view. Such expressions have been suggested for the growth under the SGS [13], but their adequacy has been questioned [14–17]. The great accuracy of description of the KMC data provided by the GD in 2D case in Ref. [11] and in the 1D case studied in the present paper is an important argument in favor of the 2SGS. Additionally, the method affords narrower distributions of both the capture zones and of the gap size distributions (in the 1D case), which can be of interest for practical applications.

Furthermore, we will show that the scaling of size distributions takes place when the deposition to diffusion rate ratio is equal to zero, the average number of atoms in the island is infinite and the spatial island extent remains constant, thus identifying the relevant variables responsible to the deviations from scaling.

The material is distributed as follows. In the next section we explain our models and notation and present results of our KMC simulations. In Sec. III we derive the results of the second-step growth in the framework of two analytic approaches; in Sec. IV we will discuss a possibility of experimental verification of our predictions, and in the last

 ©2015 American Physical Society

section we briefly summarize the obtained results and discuss their relevance to the development of the scaling theory for the SGS.

II. TWO-STEP GROWTH IN 1D MODELS

A. The models

The models of irreversible epitaxial growth are conventionally characterized by an integer number i defined as one less than the minimal number of atoms needed to nucleate a stable island [2,3]. In the present study we will restrict ourselves only to the most frequently studied case $i = 1$ when islands are nucleated at the meeting of two atoms. After nucleation, the island can only catch the atoms and grow but detachment of atoms is forbidden. With the usual restriction to the solid-on-solid growth [3] the morphology of 1D islands from the point of view of growth kinetics can be fully characterized by a single parameter, the island diameter which in one dimension coincides with the length l of the chain of the sites on the substrate covered by the island. This is because the deposited atom can either impinge directly on the island with the probability equal to the ratio of the sum of the island diameters to the total number of sites on the substrate $P_{\rm imp}$ or be deposited at the bare substrate with the probability $1 - P_{\rm imp}$.

Islands of different morphologies can be described with the use of the effective aspect ratio

$$r = h/l, \tag{1}$$

where h is an effective island height calculated as the ratio of the island size s to its diameter: $h = s/l$. The extreme cases are the submonolayer islands with $h = 1$ when all atoms are deposited directly on the substrate in the chain of length l, so that the aspect ratio $r = 1/s$ is at its minimum, and the point islands when the island diameter is equal to only one site $l = 1$ so the aspect ratio is at its maximum $r = s$. The aspect ratio for islands of arbitrary morphologies is contained within these limits

$$1/s \leqslant r \leqslant s. \tag{2}$$

The majority of our simulations will be made within the simpler point-island model (PIM), but the submonolayer case will also be discussed to gain insight into the complications brought about by this more realistic case [2–4]. The model with chainlike islands can describe some experiments on the growth of the monatomic islands [18,19], in particular, those growing at the steps of the vicinal surfaces (see Refs. [20,21] and references therein). We will discuss this possibility in more detail in Sec. IV.

B. KMC simulations

1. 2SGS protocol and physical parameters

At the first step of the 2SGS a small quantity of adatoms, which we will characterize by the initial coverage θ_0, are simultaneously placed at the substrate at random positions. Experimentally this can be achieved by a fast deposition at low substrate temperature when the surface diffusivity is negligible. Then the atoms are allowed to diffuse (the substrate temperature can be raised, if necessary) nucleating stable dimer islands when meeting another mobile atom or attaching themselves to already nucleated islands. In the absence of the deposition flux the diffusivity rate alone defines the time scale in the system. So as long as the diffusion constant D is nonzero its precise value does not matter.

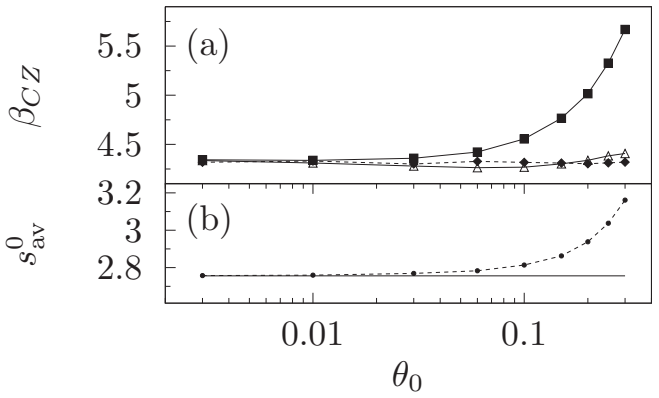

FIG. 1. (a) Symbols: the shape parameter of the GD Eq. (11) fitted to the KMC data on the CZD for the point (♦) and extended (■) islands; △, the data for extended islands fitted to the GD with the shifted argument Eq. (14); the lines are guides to the eye. (b) Points: average sizes of the extended chainlike islands nucleated from the initial random deposition with coverage θ_0; horizontal solid line: universal island size Eq. (4) for PIM.

When all mobile monomers disappear, an ensemble of small islands of average size $s^0_{\rm av}$ and the density

$$N_0 = \theta_0/s^0_{\rm av} \tag{3}$$

arises. That terminates the first growth step. A remarkable fact noted previously in the two-step growth in two dimensions is that $s^0_{\rm av}$ very weakly depends on θ_0. For example, in the case of the PIM the simulated average sizes of the nucleated islands were of practically the same size

$$s^0_{\rm av} = 2.756 \pm 0.001 \tag{4}$$

for seven values of the initial coverage in the range

$$3 \times 10^{-3} \leqslant \theta_0 \leqslant 0.3. \tag{5}$$

The value of $s^0_{\rm av}$ is shown in Fig. 1 by thin horizontal line because the statistical errors are too small to be shown on the scale of the drawing. For comparison also shown are the values of $s^0_{\rm av}$ for extended submonolayer islands. Here the finite island size grows with coverage. This is usually associated with the approach to the coalescence regime (which is absent in the PIM). Within the 2% accuracy level chosen by us in the present study the nucleated extended islands have approximately the same value of $s^0_{\rm av} \approx 2.76$ for $\theta_0 \lesssim 0.1$. We expect that our results obtained with the use of PIM could be applied at this level of accuracy also to the extended islands of different morphologies (not necessarily the linear chains) up to the coverage $\theta_0 \approx 0.1$.

At the second growth stage the experimental setup is practically the same as in the SGS, namely, the deposition of atoms at some constant rate F. The essential difference is

that the diffusion to deposition rate ratio

$$R = D/F \tag{6}$$

should be chosen in such a way that the nucleation of new islands at the surface were virtually nonexistent. To achieve this in our simulations, the growth parameters where chosen to be close to those typically found in metal epitaxy [3,7,20,22,23], namely, the deposition flux $F = 0.003$ ML/s, the deposition temperature $T = 250$ K, the activation energy of diffusion $E_d = 0.25$ eV. The diffusion constant was calculated according to the standard formula [3]

$$D = \nu \exp(-E_d/kT)/q, \tag{7}$$

where k is the Boltzmann constant, $q = 2$ the substrate coordination number, and $\nu = 10^{12}$ Hz the attempt frequency. This choice led to the value of

$$R \approx 1.5 \times 10^9 \tag{8}$$

roughly in the middle of the typical experimental range $10^5 < R < 10^{11}$ [7]. The value is large enough to ensure the absence of nucleation in all our second step growth simulations to a very good precision. Smaller values of R could have been used at the adopted level of accuracy (~2%), especially at larger island densities, but this question has not been investigated. The systems simulated were chosen to be of rather large sizes of $5-10 \times 10^5$ sites. But this was only to gather sufficiently good statistics to which end the simulation was additionally repeated multiple times to grow up to ~10^7 islands. The finite-size problems that are common under the SGS [2] did not appear in our 2SGS because at the first growth step many atoms are deposited at once. In one dimension their movements are restricted by the left and right neighbors, so they are never able to traverse the whole system, as is the case when the atoms are deposited one by one. Thus, the finite system as effectively "seen" locally by an adatom is indistinguishable from an infinite one.

To test the quality of the requirement of no nucleation on the second step with the growth parameters chosen, a test simulation of the second step growth with $\theta_0 = 0.03$ and $\theta = 1$ in the PIM was performed. The number of islands at the end of the second step was augmented only by 0.2%. But in the majority of our simulations the maximum coverage θ was an order of magnitude smaller.

2. The scaling analysis

In the case of the irreversible growth the scaling hypothesis postulates that the ISD within each universality class (characterized by i, the island morphology, etc.) can be described with the use of a function $f(x)$ defined according to the relation [1–3]

$$N_s = \frac{\theta}{s_{\rm av}^2} f(x = s/s_{\rm av}), \tag{9}$$

where N_s is the density of islands of size s, θ the total surface coverage and $s_{\rm av}$ the average island size. We omit the dependence on i and other parameters because in the present paper only the $i = 1$ case for point and linear chain islands will be studied, so in Eq. (9) $s \geqslant 2$. Also, because the scaling is expected only in some asymptotic limit at some specific "critical" values of the growth parameters (see the Introduction), we, following many authors, will plot the ISD data in the form of $f(x)$ derived from Eq. (9) in order to visualize the scaling and/or its absence.

FIG. 2. Schematic drawing showing three point islands (**A**, **B**, and **C**) separated by two gaps A_1 and A_2. Also shown is the CZ of island **B** of size $A^{\rm CZ} \simeq (A_1 + A_2)/2$.

The physics of the scaling behavior is greatly simplified in our 2SGS where nucleation is restricted only to the first growth step. If further restriction to the precoalescence stage is adopted in the case of extended islands (the phenomenon is absent in the PIM), the number of islands in the system will remain fixed throughout the whole second stage. In the PIM this further means that the distribution of interisland gaps, hence of the CZs, remains unchanged, because unlike in two dimensions, in the 1D case the CZs can be easily defined from purely geometric considerations (see Fig. 2). In the case of extended islands this will be fulfilled to a good approximation in the precoalescence regime.

The first step of the 2SGS was simulated at seven values of the initial coverage in the range given by Eq. (5) both for PIM and the chainlike islands. The distributions of gap and capture zone sizes as obtained in the simulations at $\theta_0 = 0.03$ are shown in Fig. 3 for PIM. We did not show the extended island data because at this and smaller values of the initial coverage the data virtually coincided. A more interesting observation was that both the CZDs and gap size distributions data at small θ_0 could be accurately described with the use of a dimensionless scaling function

$$G(A) = g(y = A/A_{\rm av})/A_{\rm av}, \tag{10}$$

where G is either the gap or the CZ size distribution, g the corresponding scaling function, A the gap or CZ size, and $A_{\rm av}$ its average value. It is to be noted that unlike in the SGS,

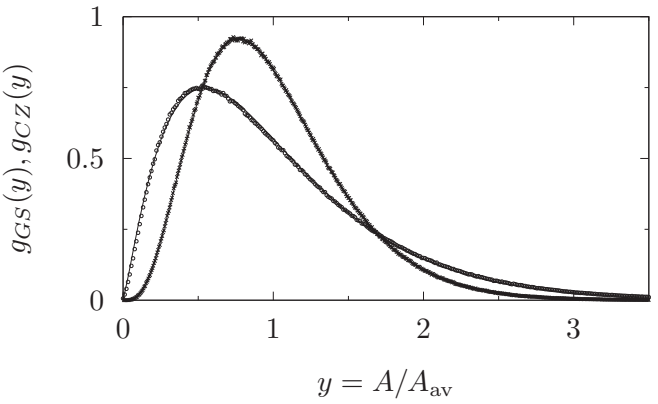

FIG. 3. KMC data for size distributions of interisland gap size (○) and the island capture zones (×) for coverage $\theta = 0.03$. Statistics were gathered over ~10^7 islands. Thin solid lines are fits to the GD Eq. (11) with $\beta_{GS} \simeq 2.19$ and $\beta_{CZ} \simeq 4.32$.

in our case the scaling of the CZDs immediately implies the ISDs scaling at the late second-step stage of growth when $s_{\rm av}$ attain large values, as will be discussed in detail in Sec. III A below.

More important is the observation, which is our main empirical finding in this paper, that, as can be seen from Fig. 3, both scaling distributions could be accurately fitted to the GD [24]

$$P_\lambda(y) = \frac{\lambda^\beta}{\Gamma(\beta)} y^{\beta-1} e^{-\lambda y} \tag{11}$$

with $\lambda = \beta$ when the scaling variable y as in Eq. (10) is used.

Now, from Fig. 2 it is seen that if we assume that the gaps between neighbor islands are not correlated, the probability distribution of the CZs (CZDs) can be obtained from the sum of two random variables that is distributed as the convolution of two gap size distributions (the contribution from the island size is constant in the PIM). But according to Fig. 3 the gaps satisfy the GD, and the convolution of two GDs is again a GD with the shape parameter equal to the sum of the individual shape parameters (see Ref. [24]). Hence, the shape parameters should satisfy

$$\beta_{CZ} = 2\beta_{GS}. \tag{12}$$

This equality is satisfied by the simulated values to the accuracy better than 2% (see caption to Fig. 3). We note that in the case of randomly distributed nucleation centers the gaps are distributed according to the exponential distribution, which is a particular case of the GD with $\beta^r_{GS} = 1$. In this case Eq. (12) gives $\beta^r_{CZ} = 2$. Because the relative width of the GD (dispersion to mean ratio) is defined solely by its shape parameter as $\beta^{-1/2}$ [24], the CZDs, gap size distributions, and, as a consequence, the asymptotic ISDs (see Sec. III A) are about 50% narrower than in the random island distribution

$$\sqrt{\frac{\beta_{GS}}{\beta^r_{GS}}} = \sqrt{\frac{\beta_{CZ}}{\beta^r_{CZ}}} = \sqrt{\frac{4.32}{2}} \simeq 1.47. \tag{13}$$

In addition, the distributions are more symmetric because the skewness of the GD scales with β also as the inverse square root [24] and thus is 50% smaller in the 2SGS in comparison with the random case. This may be of practical importance for the growth of nanoisland ensembles.

As can be seen from Fig. 1(a), at larger values of the initial coverage the values of β_{CZ} for extended and point islands diverge. While the PIM values remain constant within the statistical errors, the values for extended islands grow with coverage, thus violating the universality picture. To establish empirically the relevant variable that is responsible for the discrepancy, in Fig. 1(b) we plotted the average island size values, which behave qualitatively exactly like β_{CZ} for extended islands. This can be qualitatively understood with the use of the notion of the CZ with exclusion [25]. In Ref. [25] it was shown that if there exists the island neigborhood where other islands cannot be present, the CZD retains the GD shape but with larger value of the shape parameter β. The PIM and the extended island model differ in that the average linear size l of the point islands is equal to one site irrespective of the coverage. Because of this and of the growth kinetics adopted (see Sec. II B 1), the minimum possible average CZ is also trivially equal to unity $A^{(x)}_{\rm min} = 1$. This is the part of the CZ where the CZD should be zero. Extended islands, on the other hand, have $A^{(x)}_{\rm min} = 3$ because the smallest island with $l_{\rm min} = 2$ should be surrounded by at least one empty site at each side to form a CZ. Thus, on average the minimum CZ in this case will be $A^{(x)}_{\rm min} = s^0_{\rm av} + 1$. Thus, the CZD at small values of $y = A/A_{\rm av}$ will be suppressed on average in the case of extended islands for $A \lesssim s^0_{\rm av} + 1$. In the PIM this phenomenon is absent. The function that will be almost zero up to $s^0_{\rm av} + 1 \approx 3.76$ will have its effective value of the power-law behavior β enhanced in comparison with the PIM case.

To heuristically account for this in the scaling theory the following change of variables in the scaling ansatz was attempted:

$$y = \frac{A}{A_{\rm av}} \to y = \frac{A - \Delta l}{A_{\rm av} - \Delta l}, \tag{14}$$

where

$$\Delta l = A^{(x)}_{\rm av} - A^{(x)}_{\rm min}. \tag{15}$$

The shift in Eq. (15) is zero for the point islands because the island of any size occupies only a single lattice site, as explained above. In the case of extended 1D islands, however,

$$\Delta l_{\rm ext} = s^0_{\rm av} - 2. \tag{16}$$

With the ansatz given by Eqs. (14)–(15) it was possible to fit the KMC simulation data for extended islands with roughly the same universal value of $\beta_{CZ} \approx 4.32$ as the PIM data [see Fig. 1(a)]. Thus, we have empirically established that the average nucleated island size deviation from its minimum value Eq. (16) can be used as the relevant variable defining deviation of the CZD from its scaling asymptotics.

III. ANALYTIC TREATMENT OF THE SECOND STEP GROWTH

The scaling behavior of the CZDs and gap size distributions discussed above is fully developed already at the first growth step because at the second step the geometry of the system remains unchanged due to suppressed nucleation. In contrast, the scaling behavior of the ISDs can be observed only at the second growth step because at the first step the islands do not grow beyond very small sizes. By the definition of 2SGS, at the second step the deposition should be so slow that the nucleation was practically nonexistent and the growth was dominated by the aggregation. Because in this case the deposited atoms are distributed among a fixed number N_0 [see Eq. (3)] of already existing islands, the average island size grows linearly with the deposition time as

$$s_{\rm av} = s^0_{\rm av}\theta/\theta_0 = s^0_{\rm av}(1 + Ft/\theta_0). \tag{17}$$

The second equality follows from the fact that in the two-step growth $\theta = \theta_0 + Ft$. On the other hand, $s_{\rm av}$ is an experimentally measurable quantity, so in studying the evolution it is possible to use $s_{\rm av}$ as the evolution parameter instead of time, as will be done in the next subsection.

A. Probabilistic approach

In the absence of nucleation the evolution of the ISD can be viewed as the distribution of deposited atoms between fixed number of islands in proportion to the sizes of their CZs. This purely probabilistic problem appears also in the case of inhomogeneous nucleation at impurities studied and solved in Ref. [12]. The solution reads

$$N_j = \frac{1}{A_{\rm av}} \int_0^\infty dy g(y) \frac{(j_{\rm av} y)^j}{j!} \exp(-j_{\rm av} y). \qquad (18)$$

Here j is the number of atoms in the islands that nucleated inside the CZs of impurities with the CZD $g(y = A/A_{\rm av})$. As is seen, there exists a nonvanishing density $N_{0,1}$ of "islands" containing zero or one atom. These cases describe the impurities that did not catch any atoms at all or caught only one atom. As we argued in Ref. [11], the second step growth is a particular case of the inhomogeneous growth with the islands nucleated at the first step playing the role of the impurities. In principle, we could apply Eq. (18) to our problem by assuming that in our case each impurity has already caught on average $s^0_{\rm av}$ atoms but not less than two. Then by taking the initial atomic distribution N^0_s from our first step simulations and assuming that the number of atoms caught initially is independent of the CZ size we could solve our problem of the second step growth by probability theory means as the sum of two independent random variables that is obtained as the convolution of two distribution Eq. (18) and N^0_s.

We, however, will adopt a simpler and, arguably, more accurate route by noting that in the $i = 1$ case under the study the freshly nucleated islands contain exactly two atoms. The $s^0_{\rm av} = 2.76$ arises from the fact that some islands catch additional atoms after their nucleation. It is reasonable to assume that the probability of an atom to be trapped in the interisland gap is proportional to the gap size, and, as a consequence, the probability for an island to catch this atom is proportional to the size of its CZ (see Fig. 2). Thus, similar to the impurity case we may consider the growth as the capture of deposited atoms by the CZs that already contain two atoms as

$$N_{s\geqslant 2} = \frac{1}{A_{\rm av}} \int_0^\infty dy g(y) \frac{[(s_{\rm av} - 2)y]^{s-2}}{(s-2)!} e^{-(s_{\rm av}-2)y}. \qquad (19)$$

Now substituting here $g(y)$ of the Gamma type with the shape parameter β_{CZ} one gets [11]

$$\bar{N}_s = [(1+\xi^{-1})^{\beta_{CZ}} (1+\xi)^j j B(\beta_{CZ}, j)]^{-1}|_{j=s-2}, \qquad (20)$$

where $\xi = \beta_{CZ}/(s_{\rm av} - 2)$; the bar over the density means that it is normalized to unity. This is done by multiplying N_s [cf. Eq. (9)] with

$$A_{\rm av} = 1/N_0 = s^0_{\rm av}/\theta_0 \simeq s_{\rm av}/\theta; \qquad (21)$$

the last equality in Eq. (21) reflects the absence of the nucleation at the second growth step.

The ISDs calculated with the use of this formula are presented in Fig. 4 in the scaling form of Eq. (9). As is seen, the KMC simulations data are accurately reproduced for all relevant values of the average island size. Visually the asymptotic scaling distribution is reached already at $s_{\rm av} \lesssim 10$ at $\theta = 0.1$. This conclusion can be rigorously substantiated with the use of the Laplace method. Indeed, Eq. (18) can be cast in the form of the Laplace integral as

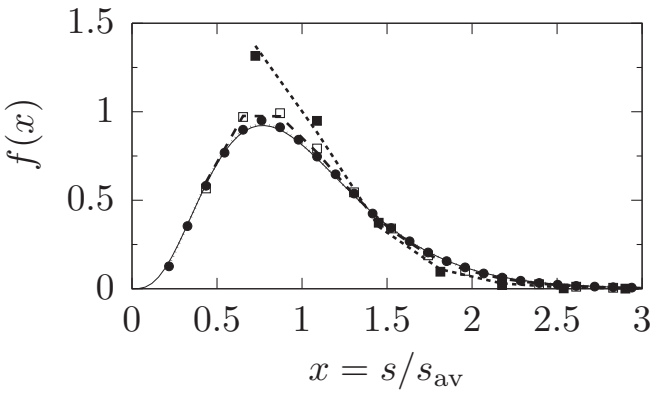

FIG. 4. Island size distributions during the two-step growth at three coverages. Filled squares, KMC simulations at $\theta = \theta_0 = 0.03$; empty squares—$\theta = 0.05$; black circles, $\theta = 0.1$. Dashed lines are drawn through the points calculated according to Eqs. (20) and/or (40), and the thin solid line is the GD [Eq. (11)] (for further explanations see the text).

$$N_s = \frac{(s_{\rm av} - 2)^{s-2}}{(s-2)!} \int_0^\infty dy g(y) \frac{e^{2y}}{y^2} \exp[-s_{\rm av}(y - x \ln y)], \qquad (22)$$

where $x = s/s_{\rm av}$. With the use of the standard means and Eq. (9) one arrives at the expected result

$$f(x) = g(x) + O(1/s_{\rm av}), \qquad (23)$$

where higher terms of the asymptotic expansion can be calculated with the use of explicit formulas given in Ref. [26]. But in the present paper we will restrict ourselves to the observation that Eq. (23) gives a rigorous proof that the average island size is a relevant variable in the scaling approach and that exact scaling can be attained only for infinitely large $s_{\rm av}$. Still, as can be seen from Fig. 4, the approach to asymptotic distribution is very fast and the scaling concept can be useful already starting from a rather modest average island sizes of about 10 atoms. For clarity the KMC data for higher coverages are not shown because on the scale of the figure they all consist of the points with the abscissa values $x = s/s_{\rm av}$ with $s_{\rm av}$ calculated according to Eq. (17) and the points lying at the solid curve corresponding to the GD [Eq. (11)].

B. Rate equations

The probabilistic approach allowed us to account for the dependence of the ISD on the average island size and to show that the scaling behavior takes place only at infinitely large value of $s_{\rm av}$. The dependence on the diffusion to deposition rates ratio R, however, was missing. But the rate equations that describe the KMC data in a qualitatively correct way do depend on both rates [2–4]. Thus, the question arises whether our probabilistic approach is compatible with the rate-equation approach. Below we will prove this using the simplest version

of the rate equations [2,3]

$$\frac{dn}{dt} = F - 2D\sigma_1 n^2 - Dn\sum_{s\geqslant 2}\sigma_s N_s, \tag{24}$$

$$\frac{dN_2}{dt} = D(\sigma_1 n^2 - n\sigma_2 N_2), \tag{25}$$

$$\frac{dN_s}{dt} = Dn(\sigma_{s-1}N_{s-1} - \sigma_s N_s), \quad s > 2, \tag{26}$$

where N_s is the density of islands of size $s \geqslant 2$, n the density of mobile monomers, σ_s is a capture number that describes the rate of attachment of mobile monomers to islands of size s [27]. In these equations we, following many authors (see, e.g., Ref. [4]), neglected for simplicity the direct impingement terms corresponding to the events when the atoms are deposited directly on the island, though these processes were present in the KMC simulations. The approximation, however, should be good at small island concentration when the surface is mostly empty, especially in the point island case when the island themselves occupy only one site. In the case of large island concentration the direct impingement may contribute significantly to the islands growth rates. In such cases the direct impingement terms should be added in Eqs. (24)–(26) [3]. But in the present paper we will restrict our study only to the small concentrations.

As is known, at large values of R the system at the aggregation stage enters into the quasistationary regime when diffusing monomers form almost time-independent profiles [2–4]. In terms of the rate equations this picture arises when the monomer density becomes small so that the quadratic terms in Eqs. (24) and (25) responsible for the island nucleation become much smaller than the aggregation terms. Nonetheless, in contrast to 2SGS, in the SGS the island nucleation cannot be neglected during the whole deposition run. The new islands appear all the time and the ISD at small island sizes remains only about two times smaller than at its maximum value [2,3]. This makes the ISD be very broad and asymmetric. Solutions of Eqs. (24)–(26) for this case have been extensively studied in the literature (the bibliography can be found in Ref. [3]) so we will not discuss them here.

In contrast to the SGS case, in the 2SGS we demand that at the second step R is set to so a large value that the nucleation could be completely neglected. In this case we may discard quadratic in n terms from Eqs. (24)–(25). With the use of new evolution parameter

$$\tau = D\int_0^t n(t)dt, \tag{27}$$

Eqs. (25)–(26) can be rewritten as

$$\frac{dN_2}{d\tau} = -\sigma_2 N_2, \tag{28}$$

$$\frac{dN_s}{d\tau} = \sigma_{s-1}N_{s-1} - \sigma_s N_s, \quad s > 2. \tag{29}$$

As is seen, Eqs. (28) and (29) constitute a closed set of linear evolution equations that in many cases admit closed-form solutions. For example, if the capture numbers are time-independent, the set can be solved with the use of the Laplace transform. In extensive KMC simulations in Refs. [6,9] it was shown that in the SGS the capture numbers do depend on time in the case of the extended islands. But CZs in SGS are also time-dependent due to the continuing nucleation. So assuming that the dependence is fully due to this fact we may assume that in our case capture numbers are constant.

Next we need to pose the initial-value problem at the beginning of the second growth step. To do this, we could take the values of island densities $N_s(\tau_1)$ at the end of the first growth step at some value $\tau = \tau_1$ which could be found by integration of Eqs. (24)–(26) from $\tau = 0$ to $\tau = \tau_1$. Three obstacles make this route quite difficult. First, Eq. (24) cannot be linearized with the substitution (27), so numerical integration would be necessary. Second, this would diminish the usefulness of the linearization of the rate equations at the second growth step. Third, we would need the values of capture numbers which in the presence of nucleation cannot be given a simple geometric interpretation so full many-body problem need be solved to find their values [27,28].

To overcome the difficulties we once again resort to the observation made by us in Ref. [29] that the ISDs can be fully characterized by the average island size $s_{\rm av}$ that effectively can replace the evolution parameter (t or τ). Thus, as in Sec. III A we assume that the aggregation starts from the freshly nucleated islands of size two as

$$N_2(s_{\rm av} = 2) = \theta_0/s_{\rm av}^0, \quad N_{s>2}(s_{\rm av} = 2) = 0. \tag{30}$$

Thus, we consider that the aggregation starts at some τ_1' when all islands are the dimers and further evolution follows Eqs. (28) and (29) with the initial values being given in Eq. (30). Because Eqs. (28) and (29) are autonomous and because neither of the evolution parameters will interest us in the future, we shift the initial value of the parameter τ by τ_1' and assume that the initial values are imposed at $\tau = 0$. Now, with the use of the Laplace transform

$$\tilde{N}_s(z) = \int_0^\infty e^{-\tau z}N_s(\tau), \tag{31}$$

Eqs. (28) and (29) can be cast in the form

$$\begin{aligned}(z+\sigma_2)\tilde{N}_2(z) &= \theta_0/s_{\rm av}^0,\\ (z+\sigma_s)\tilde{N}_s(z) &= \sigma_{s-1}\tilde{N}_{s-1}(z).\end{aligned} \tag{32}$$

As is easily seen, all $\tilde{N}_s(z)$ can be found from Eqs. (32) recursively as

$$\tilde{N}_s(z) = \frac{\theta_0}{s_{\rm av}^0\sigma_s}\prod_{k=2}^{s}\frac{\sigma_k}{z+\sigma_k}. \tag{33}$$

The Laplace transform in Eq. (33) is a rational function in z so the inverse transform could be computed analytically provided the values of the capture numbers were known. Following many authors (see, e.g., Refs. [6,30–34]) let us assume that the capture numbers can be approximated by a linear function of the island size as

$$\sigma_s = as + b, \tag{34}$$

where a and b are some constants. The liner dependence is easily justified with the use of the notion of the CZs [3,6,30]. If the capture number is proportional to the size of the CZ and the island size in its turn is proportional to the capture number,

then the capture number is proportional to the island size due to the transitivity of the proportionality relationship. With the choice [Eq. (34)] of the capture numbers, Eq. (33) can be cast into the form

$$\tilde{N}_s(z) = \frac{N_0}{aj+ac}\prod_{l=0}^{j}(al+ac)\prod_{k=0}^{j}\frac{1}{z+ak+ac}\Bigg|_{j=s-2}, \tag{35}$$

where we shifted the indexes by two with respect to Eq. (33) and introduced the new constant

$$c = 2 + b/a. \tag{36}$$

By construction, parameter a cannot be equal to zero. Therefore, all singularities in variable z in Eq. (35) are simple poles, and the residues in the last product needed for the calculation of the inverse Laplace transform can be found as

$$\frac{e^{-b\tau}}{j!a^j}\sum_{k=0}^{j}\binom{j}{k}e^{-a\tau k}(-1)^k = \frac{e^{-b\tau}}{j!}\left(\frac{1-e^{-a\tau}}{a}\right)^j. \tag{37}$$

Next we transform the first product in Eq. (35) by iterating the identity for the Gamma function

$$\Gamma(v+1) = v\Gamma(v) \tag{38}$$

as

$$\prod_{l=0}^{j-1}(l+c) = \Gamma(j+c)/\Gamma(c) \overset{j\to\infty}{\sim} j^c, \tag{39}$$

where the large-j asymptotic behavior was taken from Ref. [35]. It is to be noted that the left-hand side of this equation does not make sense for $j = 0$, while the right-hand side is equal to unity. But $j = 0$ corresponds to case $s = 2$ in Eq. (35), and in this case the product is equal to unity. Thus, the right-hand size of Eq. (39) comprises all values of j. Unifying Eqs. (37)–(39) in the expression for the inverse Laplace transform of Eq. (33) the expression for the ISD

$$\bar{N}_s = C_1 e^{-\lambda_1 j}[jB(c,j)]^{-1}|_{j=s-2} \tag{40}$$

can be obtained. With the use of Eq. (37) parameters C_1, λ_1, and c in this equation could be easily expressed through the unknown parameters a,b, and τ. To express the latter in terms of some physical quantities, we would need to solve the nonlinear Eq. (25) which is a nontrivial task. Instead, in the Appendix we show how C_1, λ_1, and c can be related to experimentally observable quantities with the use of the normalization condition for $\bar{N}_s$ and the definition of $s_{\rm av}$ and that the resulting expression coincides with Eq. (20) obtained in the probabilistic approach, provided the parameter c in Eq. (40) is equal to β_{CZ}.

It should be noted that the origin of the parameter b in Eq. (34) is not completely clear. If the capture number is proportional to the size of the CZ and the island size at large s is also proportional to this size, then b should be zero. In this case β_{CZ} will acquire value 2 [see Eq. (36)], which coincides with the shape parameter for randomly distributed islands [see discussion following Eq. (12)]. This would be a natural zero-order approximation in a mean-field treatment of the problem. Thus, the nontrivial value of b has to be attributed to interatomic correlation effects. Because b/a in Eq. (36) is equal to $\beta_{CZ} - 2 = 2.32$ and is of the same order of magnitude as the mean-field contribution, we conclude that the many-body correlations are quite strong here, which is typical for 1D systems.

Thus, Eqs. (28) and (29) can exactly reproduce the results based on the probability theory that is essentially exact when the number of the CZs is fixed, i.e., when island nucleation is suppressed. The latter will obviously violate the scaling because the scaling function $g(y)$ in Eqs. (19) and (23) will change with time and/or coverage [9]. The corrections to scaling due to the omitted terms in Eqs. (24)–(26) can in principle be found as nonlinear corrections to the exactly known solutions of the linear equations (28) and (29) in the framework of some perturbative approach. We leave this nontrivial problem for future study.

Two conclusions that can be drawn from the results of this section should be stressed. A less important conclusion is that our results confirm the qualitative reasoning of Ref. [1] that the deviations from the linear dependence of the capture numbers on the island size usually observed in the SGS (see, e.g., Refs. [3,6,9]) can be attributed to the fragmentation. In the absence of the fragmentation in our 2SGS the dependence is strictly linear.

More important conclusion concerns the rate-equation approach itself. From the probabilistic theory of Sec. III A it can be concluded that the ISD at large coverage will always reproduce the CZD that arises from the deposition at the first step. But this distribution can in principle correspond to arbitrarily placed dimer islands (e.g., if instead of our instant deposition method we used some other technique). As follows from Eq. (23), at the second step we will see the ISD corresponding to this CZD. But in the rate-equation approach all such ISDs will be characterized by the same initial value condition [Eq. (30)]. Thus, irrespective of the initial CZD the final ISD will be always the GD. This paradox is easily explained by the mean-field character of the rate equations when spatial correlations between islands are neglected. Thus, we conclude that in the general case of arbitrary CZDs a more sophisticated approach capable to take into account the spatial correlations should be used [36]. In particular, the dependence of the capture numbers on the capture area distribution revealed in Ref. [32] ought to be taken into account.

IV. EXPERIMENTAL SUGGESTIONS

One of reasons for the popularity of the notions of universality and scaling in physics are the invariance properties they reveal in physical data. In practice this means that theoretical predictions can be made that do not depend on some of experimental conditions, thus simplifying the task of their verification. As is discussed below, the values of the diffusion constant, of the deposition flux, and of the 1D surface coverage are not easily controlled in model realizations of the 1D growth. But our predictions about the average island sizes, the GD nature of probability distributions of several geometric quantities, as well as the values of the shape parameter of the GDs are universal in broad ranges of the growth conditions and thus admit experimental verification even in the absence of detailed knowledge of the growth parameters.

Theoretical predictions on 1D growth can be experimentally verified in the framework of 2D epitaxy on the vicinal surfaces with sufficiently straight step edges that can play the role of the 1D "surfaces" [22,37,38]. The realization of the 2SGS however, is not straightforward because it is not clear neither how to perform the instant random deposition at the step edge at the first growth step nor how to afford the constant deposition rate at the second step. The second task seems to be simpler because all we need is that adatoms at the steps reach the 1D islands before the next deposited adatom reaches the step edge. This in principle is achievable by adjusting the deposition rate to be so small that the time intervals between the adatoms landing at the same or nearest neighbor terraces were sufficiently long for the previously deposited atom had time to be attached to the existing step islands. On the other hand, the second-step growth is not very interesting physically. In the previous section we showed that the physics of the growth is quite transparent and easily comprehensible in the framework of the standard probability theory. Moreover, it can be described with an accuracy of about 2% within simple analytic approach.

The results of the growth during the first step, however, are not as easily grasped. We were not able to find easy explanations neither to why the average island size is independent of the initial coverage θ_0 in a broad range of its variation both in 1D and in 2D [11], nor why the interisland gaps and CZs are distributed according to the GD with the coverage-independent shape parameter in one dimension. Presumably, this is a consequence of complex many-body kinetics that would require similarly complex many-body treatment within the formalisms developed in Refs. [27,28]. Therefore, experimental check of these predictions would be of interest.

Realization of the 1D first-step growth in the 2D epitaxy could be attempted as follows, at least in some systems. We first note that the adatoms at the step edges are bound more strongly than the adatoms at the terraces because of higher coordination. This was confirmed by both *ab initio* calculations and experimental data in the case of the Ag/Pt(997) system (see Ref. [20] and references therein). Therefore, at sufficiently low temperature the detachment from the edge will be suppressed and the atoms will behave as in a true 1D system. Stronger binding at the edges can also lead to higher diffusion barrier to the edge diffusion. Therefore, at sufficiently small temperature the diffusion at the terraces can be much faster than along the steps. In this case the necessary number of atoms can be deposited at the vicinal surface at sufficiently high rate. There they will quickly reach the step edges and stay attached to them with the edge diffusion remaining negligible during the whole deposition run (2D deposition plus terrace diffusion). Now, by either annealing the system at the deposition temperature for a sufficiently long time or by slightly raising the substrate temperature to not violate the irreversibility of the step binding, it should be possible to experimentally realize the nucleation stage of the 2SGS on the step edges. *Ab initio* or least calculations could be of use in finding an appropriate system, and the growth parameters at which the scenario just described could be realized with sufficient precision in order to adequately represent the first-step growth protocol.

V. CONCLUSIONS

In this paper we studied the irreversible epitaxial growth in one dimension with the use of the KMC and the 2SGS. We showed that in contrast to the 2D case studied earlier [11], the behavior in one dimension is much simpler. In particular, in the low-coverage range usually associated with the precoalescence growth regime the shape parameter of the GD that characterized the CZDs was found to be independent of the initial seed coverage, unlike in the 2D case. Also, at the second growth step the simple 1D geometry of the CZs has made inoperative the mechanism of the narrowing of the ISDs due to the CZ boundary curvature that we saw in 2D case. As a result, the ISDs changed their form only at lower coverages attaining at higher coverages the universal GD shape with a universal value of the shape parameter. The results of the simulations at the second step for all coverages from the smallest to the largest ones could be compactly described with the use of simple analytic formulas with the accuracy of about 2%. The description comprised gap size distributions, CZDs, and ISDs, i.e., all distributions that are usually studied in the irreversible growth models and are measurable experimentally [20]. We established, in particular, that the universal value of the shape parameter of the Gamma probability distribution that describes the CZDs is more than two times larger than the value corresponding to the randomly distributed nucleation centers. This means that the distributions of the island sizes and interisland gaps are about 50% narrower than in the case of random nucleation. This is similar to the 2D case [11] and may be of interest for the growth of nanostructures of practical interest.

From an experimental point of view the universality of the CZDs and ISDs in the 2SGS in one dimension, i.e., their independence from the growth parameters in wide ranges of their variation and the simple analytic shape of the Gamma probability distribution, makes the 1D two-step growth especially convenient for experimental verification of the model. While in 2D growth or in 1D SGS the deviations of the ISDs and CZDs from those predicted by simulations can be explained by the errors in the values of the parameters, the parameter independence of the 1D two-step growth makes such an explanation untenable and allows for definite conclusions about the adequacy of the model to be drawn.

In our analytic approach we showed that a perfect scaling of the ISDs can be achieved only asymptotically for very large islands and very large values of R. Because in experiments both quantities are always finite, calculation of corrections to scaling is a task of practical interest. The finite-size corrections can in principle be calculated with the use of the Laplace method [26]. The solution of the problem of finite R is not as straightforward. A possible approach can be based on the observation that at finite R the nucleation cannot be fully suppressed. So the finite-R contributions can be sought as perturbative corrections due to the nucleation terms quadratic in n that were omitted in our treatment. Using analytic solutions of the linear problem as the zero-order approximation one can in principle be able to calculate at least the lowest order terms. Of course, the rate equations are not exact but they usually describe the behaviors in a qualitatively

correct way [3]. So after having established the qualitative form of the finite-R corrections from the rate equations one can further improve the description by fitting it either to the exact KMC simulations or by invoking a more rigorous approach [27].

It has to be stressed that in our study we used both the models and the rate equations that are conventionally used in the growth studies [2–4], only instead of the SGS, the 2SGS protocol has been used. But because the microscopic physics of the growth in both cases is the same, our approach should be applicable with some modifications also to the study of the scaling under the SGS [2–5,9]. To this end it would be necessary to first establish the scaling limit. In the simplest case of the PIM the KMC simulation results at large values of R and $s_{\rm av}$ could be numerically interpolated to the infinite values of these quantities [6]. Then the appropriate asymptotic expansion around this limit should be developed to reproduce the behavior at physical values of R and $s_{\rm av}$. The results of the asymptotic fit to the simulated data in Ref. [2] suggest that nontrivial values of the "critical indexes" could be expected. Thus, it may be hoped that with appropriately defined scaling limit and relevant variables it will be possible to build a scaling theory of the SGS along the lines discussed in the present paper.

APPENDIX: ISD AT THE SECOND GROWTH STEP

In this Appendix we show how to calculate parameters C_1 and λ_1 in Eq. (40) using the normalization of the ISD and an expression for $s_{\rm av}$. To this end we first note that the sum over the island sizes in Eq. (40) from $s=2$ to infinity is equivalent to the sum over j starting from $j=0$. With the use of the explicit expression of the Beta function through the Gamma functions with subsequent use of the integral representation for $\Gamma(\beta+j)$ and the factorial representation for $\Gamma(j)$ the following identity can be established:

$$\sum_{j=0}^{\infty} e^{-\lambda_1 j}\Gamma(j+c)/j! = \int_0^{\infty}\sum_{j=0}^{\infty}(e^{-\lambda_1}u)^j u^{c-1}e^{-u}du/j!, \times \int_0^{\infty}\exp[-(1-e^{-\lambda_1})u]u^{c-1}\,du = \Gamma(c)/(1-e^{-\lambda_1})^c. \tag{A1}$$

Thus,

$$\sum_{s=2}^{\infty}\bar{N}_s = C_1/(1-e^{-\lambda_1})^c = 1 \tag{A2}$$

[see Eq. (40)]. Taking derivative of Eq. (A1) with respect to $-\lambda_1$ and remembering that $j=s-2$ another condition is obtained:

$$\sum_{s=2}^{\infty}(s-2)\bar{N}_s = C_1 c e^{-\lambda_1}/(1-e^{-\lambda_1})^{c+1} = s_{\rm av}-2. \tag{A3}$$

From Eqs. (A2) and (A3) one gets

$$\lambda_1 = \ln\left(1+\frac{c}{s_{\rm av}-2}\right) \tag{A4}$$

and

$$C_1 = [1+(s_{\rm av}-2)/c]^{-1}. \tag{A5}$$

Thus, ISD in Eq. (40) can be fully characterized with the use of only two quantities: $s_{\rm av}$ and c. For consistency with the probabilistic expression Eq. (20) we should identify c in Eq. (40) with β_{CZ}. As to the average island size, one can use either $s_{\rm av}$ directly, in the case when experimental data provide its value, or make use of Eq. (17) to express it through other experimental quantities.

[1] T. Vicsek and F. Family, Phys. Rev. Lett. **52**, 1669 (1984).
[2] M. C. Bartelt and J. W. Evans, Phys. Rev. B **46**, 12675 (1992).
[3] J. W. Evans, P. A. Thiel, and M. C. Bartelt, Surf. Sci. Rep. **61**, 1 (2006).
[4] J. A. Blackman and P. A. Mulheran, Phys. Rev. B **54**, 11681 (1996).
[5] K. P. O'Neill, M. Grinfeld, W. Lamb, and P. A. Mulheran, Phys. Rev. E **85**, 021601 (2012).
[6] M. Körner, M. Einax, and P. Maass, Phys. Rev. B **86**, 085403 (2012).
[7] M. Einax, W. Dieterich, and P. Maass, Rev. Mod. Phys. **85**, 921 (2013).
[8] A. Pimpinelli, L. Tumbek, and A. Winkler, J. Phys. Chem. Lett. **5**, 995 (2014).
[9] M. Körner, M. Einax, and P. Maass, Phys. Rev. B **82**, 201401 (2010).
[10] K. G. Wilson and J. Kogut, Phys. Rep. **12**, 75 (1974).
[11] V. Tokar and H. Dreyssé, Surf. Sci. **637-638**, 116 (2015).
[12] V. Fournée, A. Ross, T. Lograsso, J. Evans, and P. Thiel, Surf. Sci. **537**, 5 (2003).
[13] A. Pimpinelli and T. L. Einstein, Phys. Rev. Lett. **99**, 226102 (2007).
[14] M. Li, Y. Han, and J. W. Evans, Phys. Rev. Lett. **104**, 149601 (2010).
[15] F. Shi, Y. Shim, and J. G. Amar, Phys. Rev. E **79**, 011602 (2009).
[16] A. Pimpinelli and T. L. Einstein, Phys. Rev. Lett. **104**, 149602 (2010).
[17] M. Grinfeld, W. Lamb, K. P. O'Neill, and P. A. Mulheran, J. Phys. A **45**, 015002 (2012).
[18] J. N. Crain, M. D. Stiles, J. A. Stroscio, and D. T. Pierce, Phys. Rev. Lett. **96**, 156801 (2006).
[19] J. Dorantes-Dávila and G. M. Pastor, Phys. Rev. Lett. **81**, 208 (1998).
[20] P. Gambardella, H. Brune, K. Kern, and V. I. Marchenko, Phys. Rev. B **73**, 245425 (2006).
[21] V. I. Tokar and H. Dreyssé, Phys. Rev. B **76**, 073402 (2007).
[22] P. Gambardella, M. Blanc, H. Brune, K. Kuhnke, and K. Kern, Phys. Rev. B **61**, 2254 (2000).

[23] R. Ferrando and G. Tréglia, Phys. Rev. B **50**, 12104 (1994).
[24] E. W. Weisstein, "Gamma Distribution," http://mathworld.wolfram.com/GammaDistribution.html.
[25] P. A. Mulheran and J. A. Blackman, Phil. Mag. Lett. **72**, 55 (1995).
[26] G. Nemes, Constructive Approximation **38**, 471 (2013).
[27] V. I. Tokar and H. Dreyssé, J. Stat. Mech. (2013) P06001.
[28] L.-H. Tang, J. Phys. I France **3**, 935 (1993).
[29] V. I. Tokar and H. Dreyssé, Phys. Rev. B **80**, 161403 (2009).
[30] M. C. Bartelt and J. W. Evans, Phys. Rev. B **54**, R17359 (1996).
[31] P. A. Mulheran and D. A. Robbie, Europhys. Lett. **49**, 617 (2000).
[32] M. N. Popescu, J. G. Amar, and F. Family, Phys. Rev. B **64**, 205404 (2001).
[33] F. G. Gibou, C. Ratsch, M. F. Gyure, S. Chen, and R. E. Caflisch, Phys. Rev. B **63**, 115401 (2001).
[34] J. W. Evans and M. C. Bartelt, Phys. Rev. B **63**, 235408 (2001).
[35] http://dlmf.nist.gov/5.11.E12.
[36] M. Li, M. C. Bartelt, and J. W. Evans, Phys. Rev. B **68**, 121401 (2003).
[37] A. Dallmeyer, C. Carbone, W. Eberhardt, C. Pampuch, O. Rader, W. Gudat, P. Gambardella, and K. Kern, Phys. Rev. B **61**, R5133 (2000).
[38] F. Picaud, C. Ramseyer, C. Girardet, and P. Jensen, Phys. Rev. B **61**, 16154 (2000).